Available online at www.sciencedirect.com
SCIENCE DIRECT
European Journal of Medicinal Chemistry 41 (2006) 285–295
EUROPEAN JOURNAL OF MEDICINAL CHEMISTRY
http://france.elsevier.com/direct/ejmech

Original article

In silico modelling of the interaction of flavonoids with human P-glycoprotein nucleotide-binding domain

Raj Badhan, Jeffrey Penny *

School of Pharmacy and Pharmaceutical Sciences, The University of Manchester, Oxford Road, Manchester M13 9PL, United Kingdom

Received 2 June 2005; received in revised form 14 October 2005; accepted 28 November 2005
Available online 21 February 2006

Abstract

A three-dimensional model of human ABCB1 nucleotide-binding domain (NBD) was developed by homology modelling using the high-resolution human TAP1 transporter structure as template. Interactions between NBD and flavonoids were investigated using in silico docking studies. Ring-A of unmodified flavonoid was located within the NBD P-loop with the 5-hydroxyl group involved in hydrogen bonding with Lys1076. Ring-B was stabilised by hydrophobic stacking interactions with Tyr1044. The 3-hydroxyl group and carbonyl oxygen were extensively involved in hydrogen bonding interactions with amino acids within the NBD. Addition of prenyl, benzyl or geranyl moieties to ring-A (position-6) and hydrocarbon substituents (O-*n*-butyl to O-*n*-decyl) to ring-B (position-4) resulted in a size-dependent decrease in predicted docking energy which reflected the increased binding affinities reported in vitro.

Keywords: Homology modelling; ABCB1; Nucleotide-binding domain; Flavonoid

1. Introduction

The P-glycoprotein transporter, ABCB1, a member of the ATP binding cassette (ABC) super-family of transporters, is a xenobiotic efflux pump that limits intracellular drug accumulation by active extrusion of compounds out of cells. ABCB1 possesses broad substrate specificity and substrates include members of many clinically important therapeutic drug classes, including anti-HIV protease inhibitors, calcium channel blockers used in the treatment of angina and hypertension, antibiotics and cancer chemotherapeutics [1].

The expression of ABCB1 in pharmacokinetically important tissues, particularly the intestine and liver, and in blood–tissue barriers such as the blood–brain barrier [2], means the transporter is able to influence drug absorption, tissue distribution, elimination and excretion and consequently have a major impact on the pharmacokinetic profile of many therapeutic agents.

Although existing cancer chemotherapeutic approaches are being used more effectively, treatment options for recurrent or highly drug-resistant tumours are often ineffective [3]. ABCB1 is implicated in tumour multi-drug resistance (MDR), a phenomenon whereby cells become refractory to numerous structurally unrelated chemotherapeutic drugs. ABCB1 is responsible for the active cellular efflux of drugs within at least four of the major groups of naturally occurring chemotherapeutics (anthracyclines, vinca alkaloids, taxanes and epipodophyllotoxins) and hence interacts with chemotherapeutics that are used extensively [4–6]. ABCB1 activity (resulting in reduced absorption of orally administered drugs, decreased drug penetration into brain and decreased intracellular accumulation of chemotherapeutics in tumour cells) has clinical consequences such as reduced treatment efficacy and even failure of drug-based treatment regimes. Thus, a means of effectively inhibiting ABCB1 activity in patients receiving therapeutics known to be ABCB1 substrates is an attractive means of potentially enhancing therapeutic efficacy.

Fundamental to ABCB1-mediated cellular drug efflux is the ability of the transporter to bind and hydrolyse ATP. ABCB1,

Abbreviations: ABC, ATP binding cassette; CFTR, cystic fibrosis transmembrane regulator; HIV, human immunodeficiency virus; MDR, multi-drug resistance; NBD, nucleotide-binding domain; PDB, protein databank; QSAR, quantitative structure activity relationship.

* Corresponding author. Tel.: +44 161 275 8344; fax: +44 161 275 2396.
E-mail address: jeffrey.penny@manhester.ac.uk (J. Penny).

0223-5234/$ - see front matter © 2006 Elsevier SAS. All rights reserved.
doi:10.1016/j.ejmech.2005.11.012

as with many ABC transporters, possesses an architecture of intracellular nucleotide-binding domains (NBDs) and transmembrane domains. The NBDs contain three distinct motifs, Walker A, Walker B and the Signature or C motif. The Walker A motif, also known as the P-loop, interacts with the phosphates of nucleotide di- and tri-phosphates. The function of the Walker B sequence is less clear, but it is thought to be involved in Mg^{2+} coordination within the transporter and in polarising water molecules, the activating species for hydrolysis [7]. The precise function of the Signature motif is unknown. However, mutations within this region lead to loss of transport and it is thought the motif is important in conducting the energy released from ATP hydrolysis to the transmembrane domains, thereby producing a conformational change leading to translocation of substrates across the membrane [8]. It has also been postulated that the Signature motif may function as a γ-phosphate sensor, detecting the presence of the γ-phosphate of ATP in the opposing monomer within a dimeric NBD structure [9].

Thus, since ATP binding and hydrolysis within NBDs are crucial for maintaining ABCB1-mediated drug translocation, disruption of these processes is potentially a powerful means of inhibiting transporter activity.

Plant polyphenols, specifically flavonoids (Fig. 1), occur in abundance in many of the foods and drinks that are consumed on a regular basis.

They are found in high levels in fruits, vegetables, nuts, wine and tea and intake can be up to several hundred milligrams a day. A number of studies documenting their use have reported positive effects on human health due to their antioxidant, anti-inflammatory, antiviral and anticancer properties [10]. Flavonoids have been shown to interact with NBDs of ATPase transporters and inhibit ATPase activity [11–15] and direct binding of flavonoids to the C-terminal NBD (NBD2) of murine Abcb1 has been demonstrated using saturation transfer difference-NMR spectroscopy [16]. Thus, NBDs represent potential targets for therapeutic intervention and the use of flavonoids as potential modulators of ABCB1-mediated drug efflux is highly attractive.

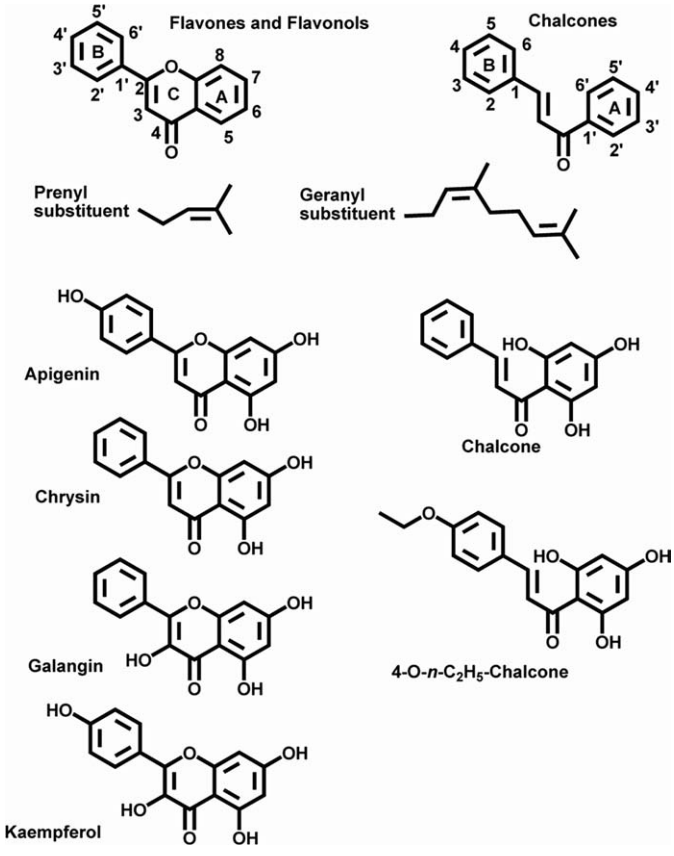

Fig. 1. Structure of flavonoids.

In silico screening of chemical entities represents a powerful and rapid approach for identification and selection of potential lead compounds prior to in vitro and in vivo studies. However, at present, the crystal structure of ABCB1 is available at a resolution of only 8 Å [17], which is insufficient to allow analyses of the mechanism of interaction of flavonoids with ABCB1 NBDs. To address this we have generated an in silico homology model of the C-terminal ABCB1 NBD (NBD2) of human P-glycoprotein and correlated the docking characteristics of a series of flavonoids and flavonoid-derivatives with the findings of in vitro functional studies and crystallographic data.

2. Results

2.1. Template identification

A BLAST search filtered for known 3D structures indicated that, to date, NBD2 of the human ABCB1 transporter demonstrated greatest homology with the C-terminal NBD of the human TAP1 transporter (PDB code: 1JJ7) [18]. Over the 249 amino acids comprising the NBD there was 46% sequence identity between ABCB1 and TAP1 (Fig. 2).

The NBD of *E. coli* haemolysin B (PDB code: 1MT0) [19], a protein transporter; the *L. lactis* MDR ABC transporter NBD (PDB code: 1MV5) [20]; the *S. typhimurium* histidine permease transporter NBD (PDB code: 1B0U) [21] and the *M. jannaschii* MJ0796 ABC transporter NBD (PDB code: 1L2T) [22] possessed between 25% and 46% homology with human ABCB1 NBD2 and were employed as templates for homology modelling since it is generally accepted that a sequence identity above 25% leads to reasonable homology models [23].

2.2. Template sequence homology and model secondary structure

Multiple sequence alignment revealed a high level of homology between ABCB1 NBD2 and the NBDs of other ABC proteins, particularly within the Walker A, Walker B, Signature sequence and Q-loop regions (Fig. 2). Within all template sequences Gly1070, Gly1073 and the GKST (1075–1078) residues of the Walker A sequence were invariant, as were SGGQ (1177–1180) Gln1182, ARA (1187–1189) within the Signature sequence and Asp1200, Thr1203, Leu1206 and Asp1207 residues within the Walker B motif.

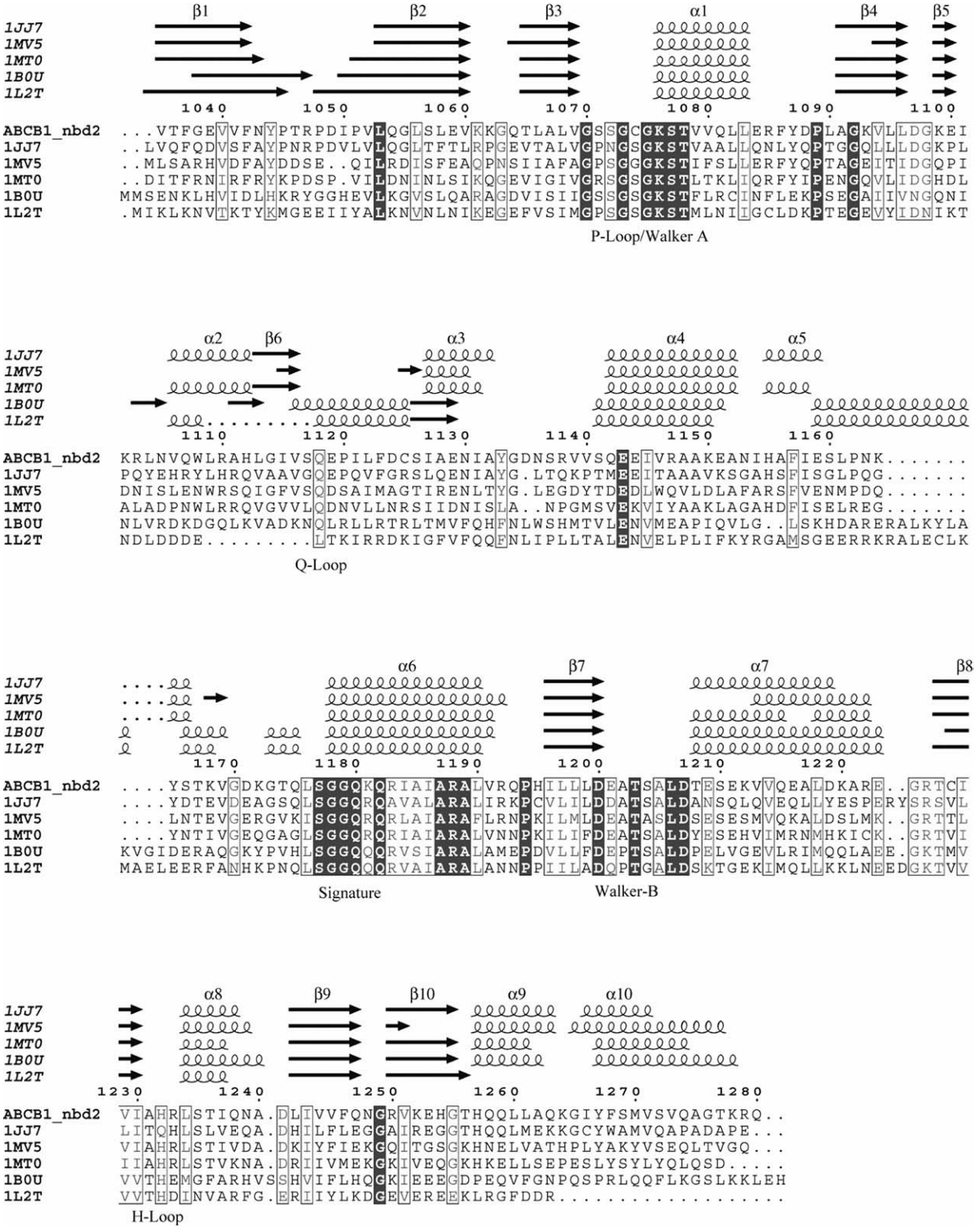

Fig. 2. Multiple sequence alignment of the NBD of ABCB1 and five homologous sequences from a BLAST search. The NBDs of: the human TAP1 (PDB code: 1JJ7), the *E. coli* haemolysin B (PDB code: 1MT0), an MDR transporter from *L. lactis* (PDB code: 1MV5), the *S. typhimurium* histidine permease (PDB code: 1B0U) and the bacterial MJ0796 transporter (PDB code: 1L2T). α-Helices, numbered helices; β-sheets, numbered arrows. Grey shaded alignments represent highly conserved residues whilst those enclosed in grey boxes signify conserved residues.

Our studies correlate in silico data derived from human ABCB1 NBD2 with in vitro experimental data of the interaction between flavonoid and murine Abcb1 NBD2. Pair wise sequence alignment between human (NCBI accession number: AAA59575) and murine (NCBI accession number: P06795) NBD2s revealed 92% sequence identity (data not shown). Moreover, residues within human ABCB1 NBD2 that are predicted to interact with flavonoids are identical in murine Abcb1

NBD2 (human Tyr1044, Ser1072, Lys1076, Ser1077 and Thr1078; murine Tyr1042, Ser1070, Lys1074, Ser1075 and Thr1076). The extremely high homology between the two NBDs and preservation of key residues that are predicted to be involved in the interaction of NBD with flavonoids supports the correlation of our in silico data with available experimental K_d data.

The overall fold pattern and topology of the ABCB1 NBD2 resembles those of the TAP1 NDB and the other NBDs templates used. We observed a total of 10 β-sheets within ABCB1 NBD2. Two anti-parallel β-sheets (β1–β2), often termed the anti-parallel-β-sheet domain, were located at the N-terminal of the NBD, six β-sheets were within a central domain with a further two located within the α-helical domain, as illustrated in Fig. 3a. Similarly the TAP1 NDB contains 10 β-sheets forming similar domains. A total of 10 α-helices were observed in the model with α-helices α2–α5 making up a discrete domain, termed the α-helical domain (Fig. 3a) as is observed in TAP1.

The presence of a cavity within ABCB1 NBD2, formed in part by the P-loop, and predicted to possess Tyr1044 and His1232 at opposing ends, is shown in Fig. 3b.

2.3. Stereochemical validation of ABCB1 NBD2 model

The bond angle stereochemistry of the ABCB1 NBD2 model determined using PROCHECK was analysed by Ramachandran plot. The latter revealed approximately 98% of NBD2-amino acids were within allowed areas (data not shown).

2.4. Prediction of the potential interactions of flavonoids with ABCB1 NBD2

Although a limited amount of in vitro functional data are available concerning interaction of flavonoids and flavonoid-derivatives with recombinant murine NBD2, little is known of the actual mechanisms of interaction between flavonoids and NDBs. To investigate the potential interaction mechanisms we sought to correlate the binding energies obtained from docking a series of 24 flavonoids and flavonoid-derivatives (Table 1) into our ABCB1 NBD2 model with published experimental K_d and crystallographic data. A correlation coefficient of 0.67 was obtained between predicted final docked energy and in vitro K_d values.

2.5. The influence of ring-B hydroxylation on flavonoid–NBD2 interaction

The flavones chrysin and apigenin (Fig. 1) are predicted to adopt potentially identical orientations within ABCB1 NBD2 and possess similar predicted docking energies (E_d) (Table 1). The orientations are such that ring-A is located within the P-loop (Gly1070-Thr1078) (Fig. 4a) with the 5-hydroxyl group involved in hydrogen bonding interactions with Lys1076 (Fig. 4b). Ring-B is predicted not to undergo hydrophobic stacking interactions with Tyr1044. Chrysin is structurally similar to apigenin as is galangin to kaempferol but chrysin and galangin both lack the 4′-hydroxyl group (Fig. 1). Our results suggest the 4′-hydroxyl group of apigenin and kaempferol potentially does not interact with Tyr1044 and has only a minimal effect on predicted docking energies (ΔE_d) for chrysin and apigenin ($\Delta E_d = 0.4$ kcal/mol) and galangin and kaempferol ($\Delta E_d = 0.39$ kcal/mol) (Table 1).

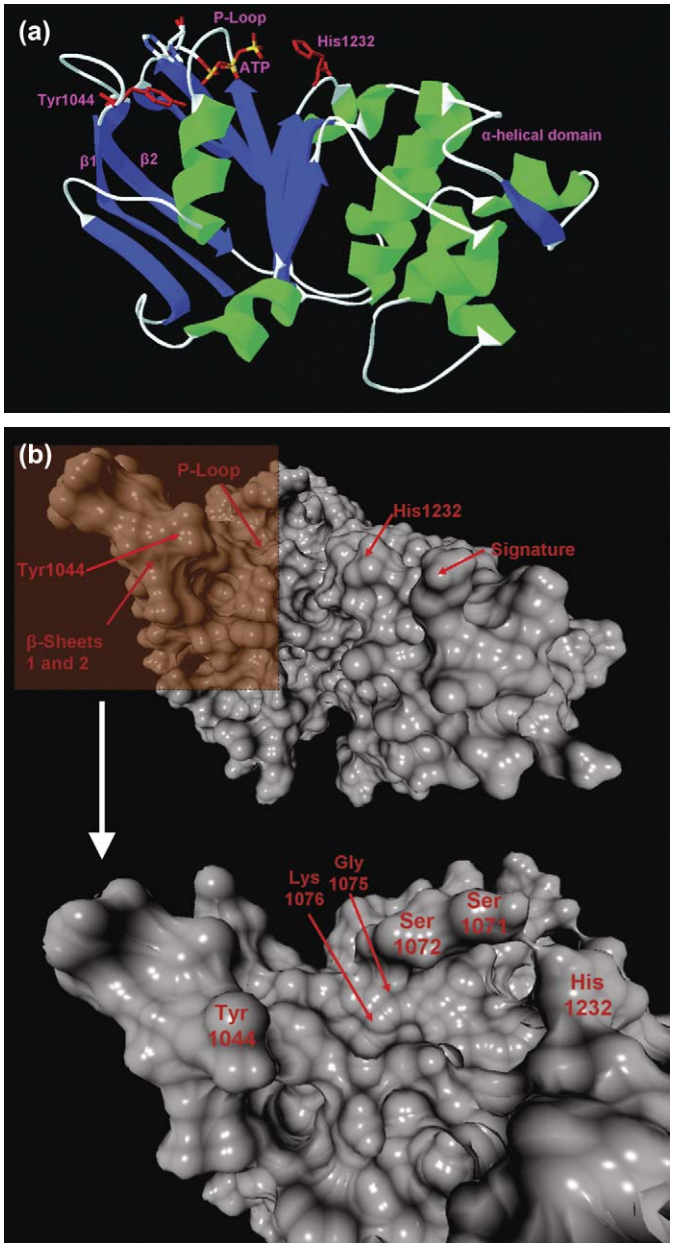

Fig. 3. (a) Three-dimensional model of the human ABCB1 NBD2 encompassing ATP within the P-loop of the NBD. Residues important for interactions with flavonoids are shown in red. (b) Three-dimensional surface representation of ABCB1 NBD2 (upper panel) with detailed surface representation of the P-loop region (lower panel).

2.6. Influence of ring-A alkylation on flavonoid–NBD2 interaction

The addition of prenyl, benzyl or geranyl moieties to position 6 of ring-A of the parent flavone was associated with a

Table 1
Predicted docking energy and experimentally determined dissociation constants for flavonoids and flavonoid-derivatives

Flavonoid group	E_d (kcal/mol)	K_d (μM)	Total cluster number	Energy range (kcal/mol)	Conformations within cluster
Flavones					
Chrysin	–7.58	8.90 ± 0.30 [30]	7	–7.85 to –7.52	56
Apigenin	–7.98	10.10 ± 1.90 [30]	4	–7.98 to –7.78	78
6-Geranyl chrysin	–12.00	0.05 ± 0.005 [30]	12	–12.00 to –10.87	22
8-Grenyl chrysin	–11.90	0.03 ± 0.005 [30]	18	–11.90 to –10.70	22
6-Prenyl chrysin	–8.74	0.30 ± 0.03 [30]	3	–8.74 to –8.61	79
6-Benzyl chrysin	–9.93	0.34 ± 0.04 [30]	2	–9.93 to –9.71	67
Tectochrysin	–7.80	6.30 ± 4.30 [30]	9	–7.80 to –7.64	19
Flavonols					
Kaempferol	–8.99	6.70 ± 0.03 [27]	4	–8.99 to –8.70	96
Quercetin	–8.50	7.00 ± 0.50 [27]	26	–8.50 to –8.36	26
Galangin	–8.60	5.30 ± 0.10 [27]	7	–8.60 to –8.37	73
Kaempferide	–9.11	4.50 ± 0.20 [27]	8	–9.11 to –8.80	60
6-Prenyl galangin	–10.16	0.21 ± 0.06 [27]	4	–10.16 to –9.99	69
8-Prenyl galangin	–10.44	0.22 ± 0.05 [27]	3	–10.44 to –10.01	58
4-*n*-C_8H_{17}-galangin	–11.50	0.06 ± 0.02 [27]	22	–11.50 to –9.95	17
2′,4′-Dichloro galangin	–9.20	4.00 ± 0.23 [27]	9	–9.20 to –8.70	44
Flavanones					
Silybin	–8.31	6.80 ± 0.30 [32]	15	–8.31 to –8.08	20
Dehydrosilybin derivatives					
Dehydrosilybin	–9.13	2.20 ± 0.10 [32]	23	–9.13 to –7.94	14
Chalcones					
Chalcone	–8.14	4.60 ± 0.30 [31]	26	–8.14 to –7.79	26
4-Hydroxy-chalcone	–8.27	4.80 ± 0.50 [31]	14	–8.27 to –7.98	45
4-O-*n*-C_2H_5 chalcone	–8.78	2.10 ± 0.20 [31]	30	–8.74 to –8.62	30
4-O-*n*-C_4H_9 chalcone	–9.71	1.00 ± 0.08 [31]	13	–9.71 to –8.13	54
4-O-*n*-C_6H_{13} chalcone	–10.57	0.27 ± 0.05 [31]	20	–10.57 to –8.81	38
4-O-*n*-C_8H_{17} chalcone	–11.75	0.02 ± 0.04 [31]	22	–11.75 to –9.64	22
4-O-*n*-$C_{10}H_{21}$ chalcone	–12.76	0.06 ± 0.04 [31]	31	–12.76 to –10.25	17

decrease in predicted docking energy. Addition of a prenyl moiety to chrysin reduced E_d as illustrated in Table 1. Associated with prenylation was an increase in the extent of hydrogen bonding, with the 5-hydroxyl group involved in hydrogen bonding interactions with both Lys1076 and Ser1077, the 7-hydroxyl group interacting with Ser1072 and the carbonyl oxygen interacting with Ser1077 and Thr1078 (Fig. 5a). Ring-B of the alkylated flavone was predicted to be adjacent to Tyr1044 and to undergo hydrophobic interactions with the residue (Fig. 5b). Addition of a benzyl group to chrysin reduced the predicted docking energy ($\Delta E_d = 2.35$ kcal/mol) whilst the greatest decrease was observed with the addition of a geranyl moiety, which substantially reduced the predicted docking energy ($\Delta E_d = 4.42$ kcal/mol), see Table 1. Similarly, addition of a geranyl moiety at position 8 reduced predicted docking energy ($\Delta E_d = 4.32$ kcal/mol). The potential surface binding modes of chrysin and 6-geranyl chrysin within ABCB1 NBD are shown in Fig. 5c. Addition of a geranyl substituent to yield 6-geranyl chrysin resulted in a predicted reorientation of the flavone within the NBD, such that a greater potential exists for interactions between the carbonyl oxygen and 5-hydroxyl group of the flavone and residues within the P-loop. The trend in reduction of predicted docking energy with addition of hydrocarbon substituents to ring-A was also observed with the flavonol galangin (Table 1).

2.7. The influence of ring-C hydroxylation on flavonoid–NBD2 interaction

Flavonols differ structurally from flavones by virtue of a 3-hydroxyl group positioned on ring-C (Fig. 1). Our studies predicted the formation of only a single hydrogen bond when the flavone chrysin was docked into our model (Fig. 4b). Addition of a 3-hydroxyl group to chrysin to yield the flavonol galangin slightly reduced the predicted docking energy ($\Delta E_d = 1.02$ kcal/mol). This 3-hydroxyl group of ring-C was predicted to be involved in hydrogen bonding, interacting with the Ser1071, Cys1074 and Gly1075 residues within the NBD (Fig. 6a). The small contribution of the 3-hydroxyl group to flavonoid interaction with the NBD is also highlighted when comparing the predicted docking energies of the flavone apigenin with the flavonol kaempferol ($\Delta E_d = 1.01$ kcal/mol), where the 3-hydroxyl group is predicted to be involved in hydrogen bonding with Cys1074, Gly1075 and Lys1076 (Fig. 6b). As with the predicted docking orientations of flavone (chrysin) and alkylated flavone (6-prenyl chrysin), ring-B of

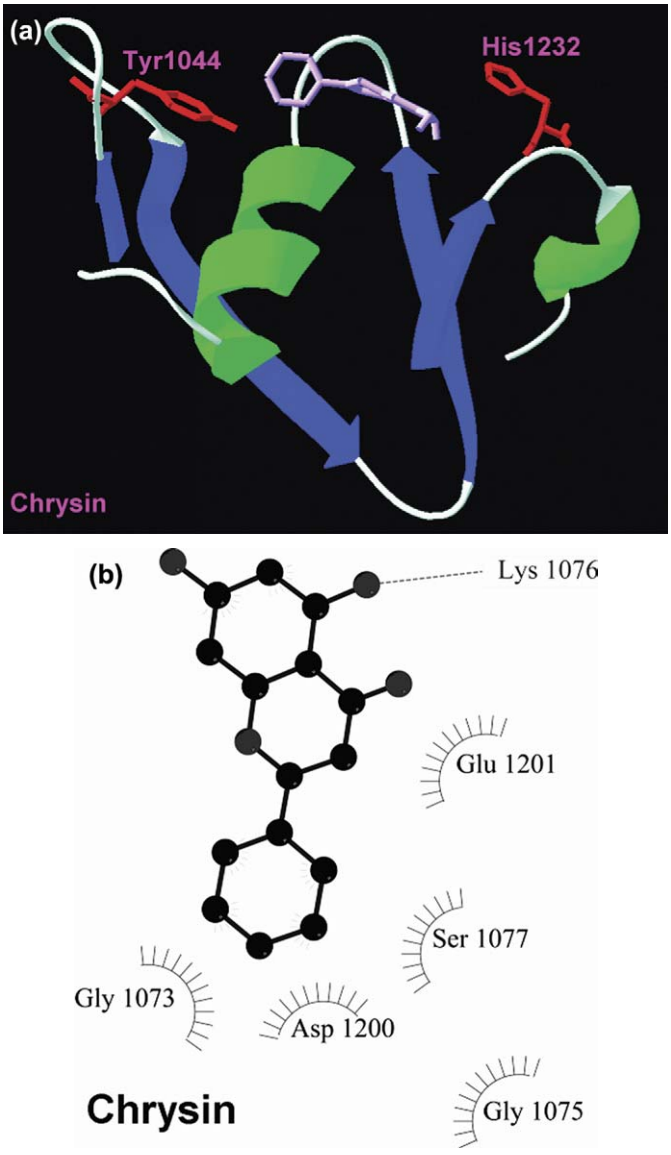

Fig. 4. (a) Three-dimensional model of the human ABCB1 NBD2 showing the docking orientation of chrysin in pink, with Tyr1044 and His1232 illustrated in red. α-Helices are illustrated by green ribbons and β-sheets are illustrated by blue arrows. (b) LigPlot interaction map of chrysin with ABCB1 NBD2. Hydrophobic interactions are illustrated by spokes and hydrogen bonding interactions by dashed lines.

kaempferol was predicted to be positioned adjacent to Tyr1044 (Fig. 6c). The reductions in docking energies reported above (ΔE_d of approximately 1 kcal/mol) are small but reflect similar reductions in experimentally determined dissociation constants [27,30,32], and suggest the 3-hydroxyl substituent is of significantly lesser importance in the overall affinity for the P-loop when compared to the effects of ring-A alkylation.

2.8. Predicted interactions of chalcones with ABCB1 NBD2

Unlike flavones and flavonols, flavonoids belonging to the class known as chalcones possess an open ring-C structure which allows for greater flexibility of the compounds within the NBD.

Ring-A of chalcone was predicted to be potentially stabilised by hydrophobic interaction with Tyr1044 with the carbonyl oxygen orientated towards the P-loop and predicted to form hydrogen bonds with Ser1077 and Thr1078 (Fig. 7a).

The carbonyl oxygen of 4-hydroxychalcone was also predicted to interact with Ser1077 and Thr1078 residues within the P-loop whereas the carbonyl oxygen of 4-O-*n*-C_2H_5-chalcone interacted with Lys1076 (data not shown). The 4-O-*n*-C_2H_5-moiety was accommodated within a cavity produced by the P-loop (Gly1070-Thr1078), Walker B (Asp1200 and Glu1201) and His1232. Addition of larger hydrocarbon substituents (O-*n*-butyl to O-*n*-decyl) at the 4-position of ring-B resulted in a decrease in predicted docking energy that was dependent upon the size of the alkyl chain attached (Table 1). Molecules possessing these larger hydrocarbon substituents exhibited similar predicted docking orientations to one another within the NBD but this orientation was reversed compared to the docking orientations of chalcone, 4-hydroxychalcone and 4-O-*n*-C_2H_5-chalcone. In this reversed orientation the alkyl group was positioned within a cavity formed by Ile1050-Val1052, Ser1072-Cys1074 and Gln1247-Gly1249. The predicted surface binding modes of chalcone and 4-O-*n*-$C_{10}H_{21}$ chalcone within ABCB1 NBD2 are illustrated in Fig. 7b. Tyr1044 (and other residues dependent on alkyl chain length) was predicted to stabilise both the alkyl group and ring-B (Fig. 7c).

3. Discussion

The high degree of sequence identity between the templates employed in this study has allowed the generation of a stereochemically valid model of ABCB1 NBD2 with 98% of residues within allowed regions as determined by Ramachandran plot. This is to be expected since NBDs contain Walkers A and B sequences and the C-motif, which represent the key domains of a functional NBD, and are extremely highly conserved within the ABC super-family.

The results obtained from our in silico docking studies are supported by measurements of flavonoid affinity for Abcb1 NBD2 obtained in vitro. When correlating predicted binding affinity with in vitro K_d data for 24 compounds we obtained a correlation coefficient of 0.67. This suggests the in silico ABCB1 NBD2 model is robust and able to predict potential flavonoid–NBD interactions since a coefficient of 0.6, or greater, has been routinely used for homology-based models used in QSAR studies [24–26]. However, it should be noted that the in vitro flavonoid–NBD binding studies using recombinant murine Abcb1 NBD2 employed a form of NBD2 (Tyr1044-Thr1224) which lacked the initial N-terminal segment within anti-parallel β-sheet1 [27–33]. The lack of N-terminal residues within anti-parallel β-sheet1 may influence dissociation constants determined in vitro as our model suggests the Tyr1044 residue plays an important role in stabilising flavonoids within the NBD. In addition, correlation between in silico and in vitro data may be influenced by the fact the in vitro K_d data have, in some instances, relatively large variability (e.g. K_d of 4-O-*n*-

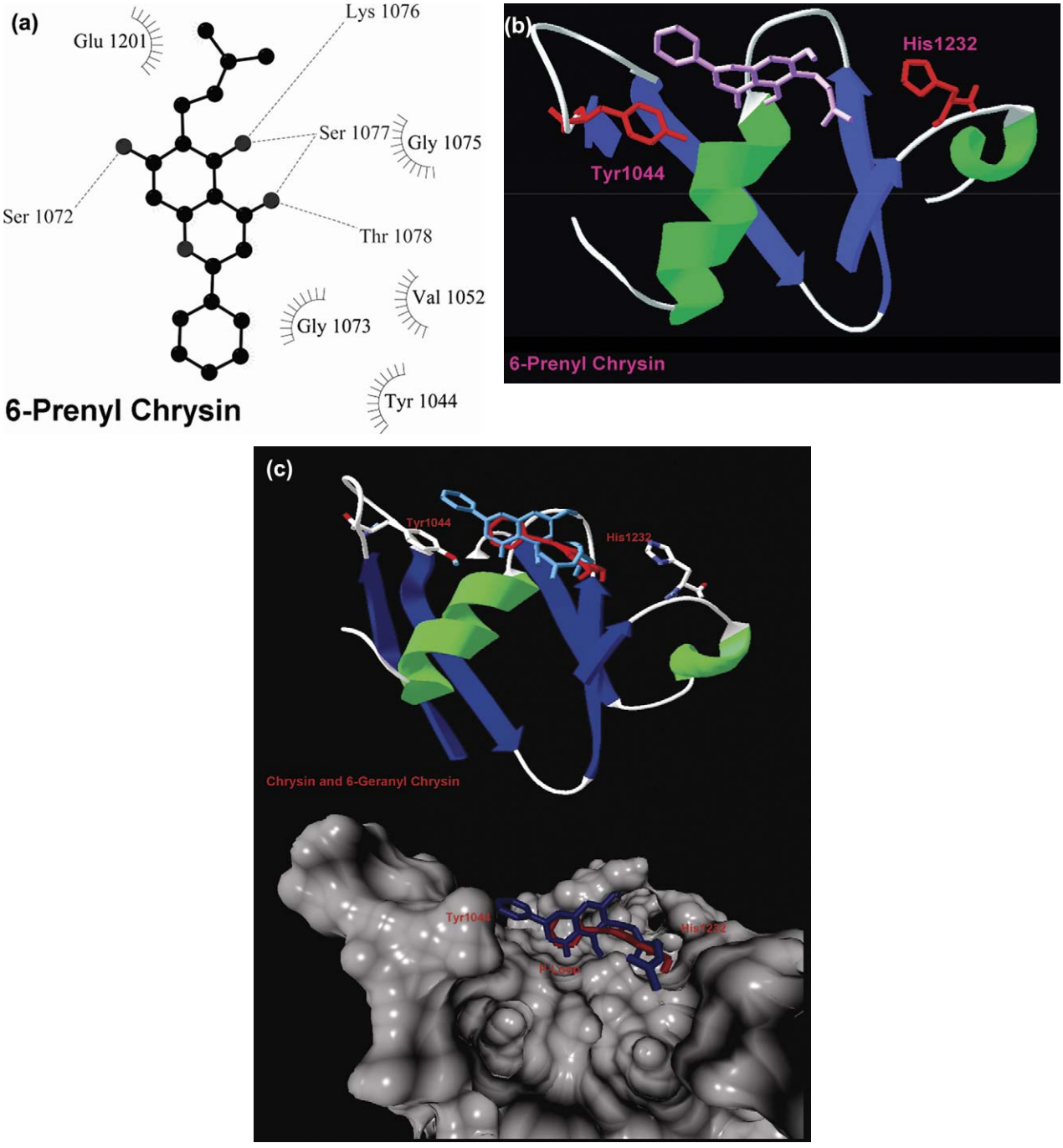

Fig. 5. (a) LigPlot interaction map of 6-prenyl chrysin with ABCB1 NBD2. Hydrophobic interactions are illustrated by spokes and hydrogen bonding interactions by dashed lines. (b) Three-dimensional model of the human ABCB1 NBD2 showing the docking orientation of 6-prenyl chrysin in pink, with Tyr1044 and His1232 illustrated in red. α-Helices are illustrated by green ribbons and β-sheets are illustrated by blue arrows. (c) Three-dimensional model (upper panel) of the human ABCB1 NBD2 showing the docking orientation of chrysin in red and 6-geranyl chrysin in light blue, with Tyr1044 and His1232 illustrated. α-Helices are illustrated by green ribbons and β-sheets are illustrated by blue arrows. Three-dimensional surface representation (lower panel) with chrysin in red and 6-geranyl chrysin in blue.

C_8H_{17} chalcone being 0.02 ± 0.04; K_d of 4-O-*n*-$C_{10}H_{21}$ chalcone 0.06 ± 0.04) making it difficult to assign a rigid rank to the binding affinities.

The flavones chrysin and apigenin exhibit potentially identical predicted orientations within ABCB1 NBD2 and possess similar predicted docking energies. These findings are consistent with those of de Wet et al. [29] and Di Pietro et al. [30] who report only a very small difference in K_d values for apigenin, 10.1 ± 1.9 μM, and chrysin, 8.9 ± 0.3 μM using recombinant murine NBD2. Further studies support this since Bois et al. [32] report similar dissociation constants for chalcone and 4-hydroxychalcone of 4.60 ± 0.30 and 4.80 ± 0.50 μM, respectively.

Addition of prenyl, benzyl and geranyl moieties at position 6 of chrysin greatly reduced predicted docking energy; substitution at the 8-position also reduced docking energies (Table 1). These findings suggest substitution at either position may po-

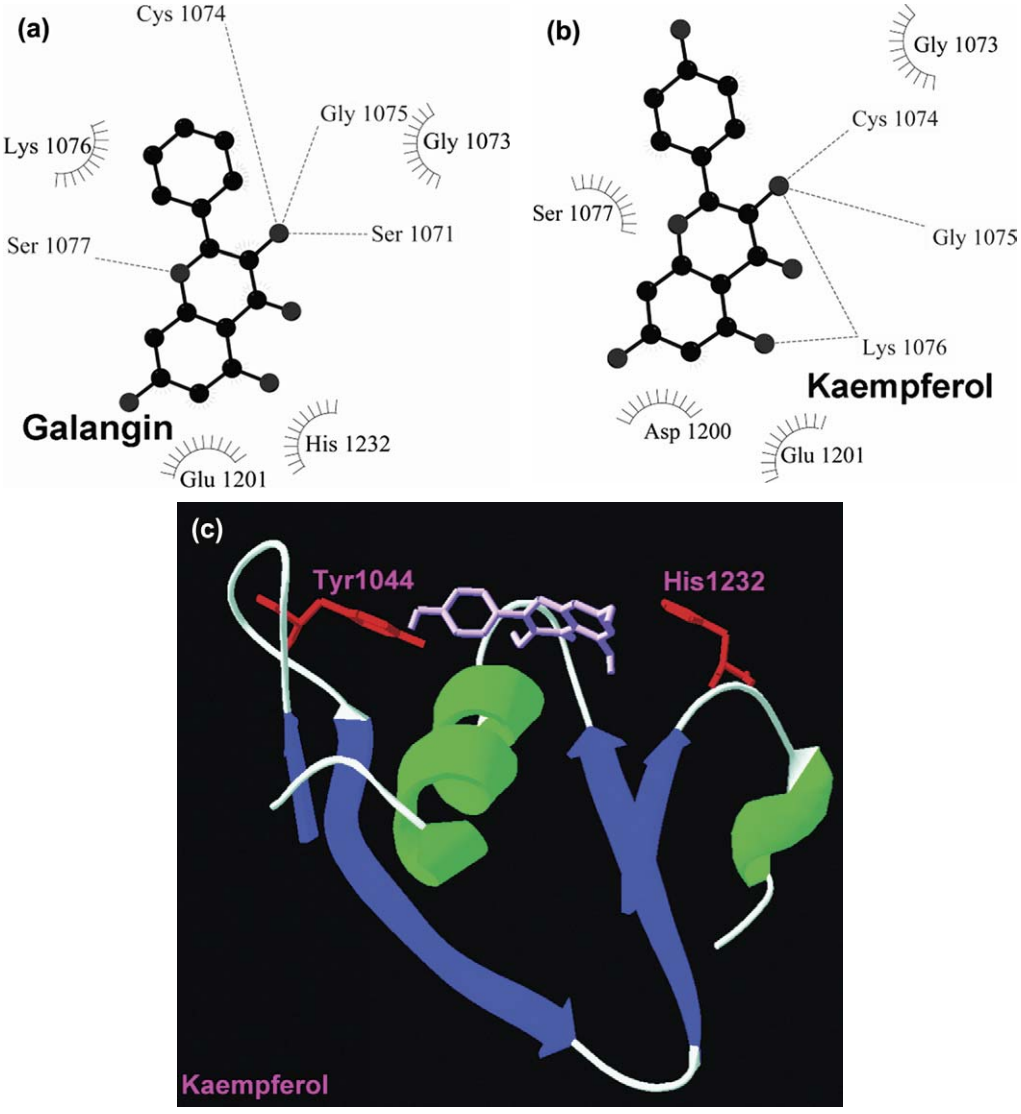

Fig. 6. (a) LigPlot interaction map of galangin with ABCB1 NBD2. Hydrophobic interactions are illustrated by spokes and hydrogen bonding interactions by dashed lines. (b) LigPlot interaction map of kaempferol with ABCB1 NBD2. Hydrophobic interactions are illustrated by spokes and hydrogen bonding interactions by dashed lines. (c) Three-dimensional model of the human ABCB1 NBD2 showing the docking orientations of kaempferol in pink, with Tyr1044 and His1232 illustrated in red. α-Helices are illustrated by green ribbons and β-sheets are illustrated by blue arrows.

tentially enhance stability within the NBD when compared to unsubstituted flavonoid. This is supported by the findings of Comte et al. [31] who report a highly significant increase in NBD binding affinity for both 6- and 8-geranyl-chrysin, $K_d = 0.05 \pm 0.005$ μM ($E_d = -12.0$ kcal/mol) and 0.03 ± 0.005 μM ($E_d = -11.9$ kcal/mol), respectively, compared to unsubstituted flavonoid, $K_d = 8.9 \pm 0.3$ μM ($E_d = -7.58$ kcal/mol). Similar reductions in predicted docking energy were observed with 6- and 8-substituted galangin (Table 1), which are also consistent with the increases in binding affinity measured in vitro using recombinant NBD2 [31].

Conversion of flavone to flavonol (chrysin to galangin and apigenin to kaempferol), by introduction of a 3-hydroxyl group onto ring-C, was associated with a small decrease in predicted docking energy and an increase in the extent of hydrogen bonding, suggesting an increase in potential binding affinity at the NBD. These findings are consistent with those of Boumendjel et al. [28] who report reduced dissociation constants for flavonols compared to flavones, e.g. apigenin 10.10 ± 1.90 μM; kaempferol 6.70 ± 0.30 μM.

Chalcone, 4-hydroxychalcone and O-*n*-C_2H_5 chalcone potentially adopt orientations whereby Tyr1044 is involved in the stabilisation of ring-A. The O-*n*-C_2H_5 substituent at position 4 of ring-B is positioned within the His1232 containing cavity and decreases the predicted docking energy. However, when chain length increases to four carbons or greater the His1232 containing cavity cannot accommodate the side chain and the substituted chalcone adopts an alternative orientation and is accommodated within a cavity formed by Ile1050-Val1052, Ser1072-Cys1074 and Gln1247-Gly1249. The particular residues within this cavity that are predicated to stabilise the O-alkyl group within the NBD are dependent on chain length. This alteration in orientation of substituted chalcone within the NBD is predicted to increase the extent of the hy-

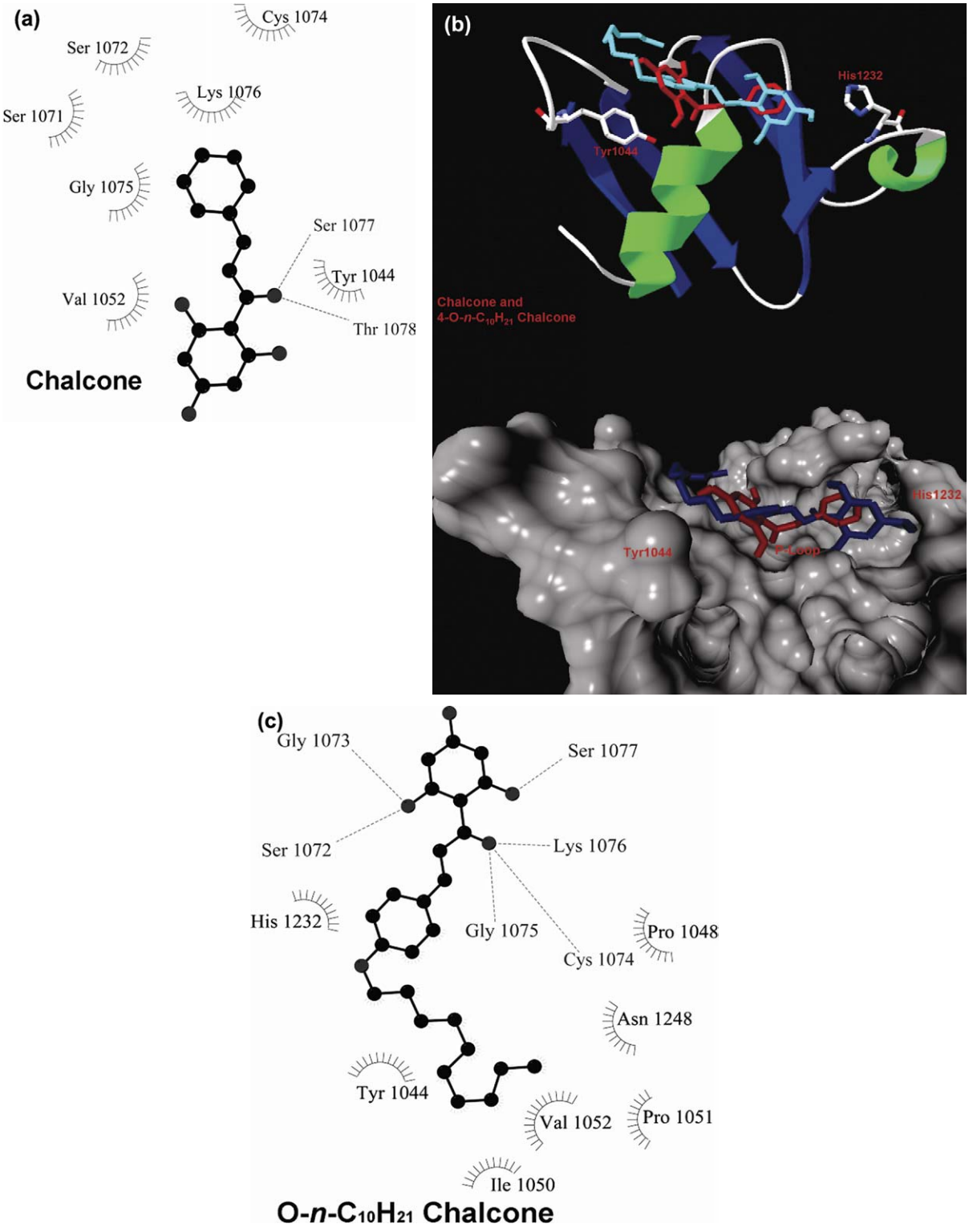

Fig. 7. (a) LigPlot interaction map of chalcone with ABCB1 NBD2. Hydrophobic interactions are illustrated by spokes and hydrogen bonding interactions by dashed lines. (b) Three-dimensional model of the human ABCB1 NBD2 showing the docking orientation of chalcone in red and O-*n*-$C_{10}H_{21}$ chalcone in light blue. α-Helices are illustrated by green ribbons and β-sheets are illustrated by blue arrows (upper panel), with the corresponding three-dimensional surface representation illustrated in the lower panel. (c) LigPlot interaction map of O-*n*-$C_{10}H_{21}$-chalcone with ABCB1 NBD2. Hydrophobic interactions are illustrated by spokes and hydrogen bonding interactions by dashed lines.

drogen bonding network between flavonoid and NBD and leads to substantial decreases in predicted docking energy (Table 1).

Hydrophobic substitution of flavonoids led to a reduction in predicted docking energy, with addition of O-*n*-$C_{10}H_{21}$ and geranyl moieties producing the greatest decreases. A similar

trend was observed by Bois et al. [32] and Maitrejean et al. [33] who reported addition of these moieties to flavonoids produced significant decreases in dissociation constants, reflecting significant changes in flavonoid binding affinity for the NBD.

Our studies suggest that flavones and flavonols are potentially orientated within ABCB1 NBD2 such that ring-B is located in a similar manner to the adenine base of ATP and is involved in hydrophobic interactions with Tyr1044. This finding is consistent with numerous studies in which ABC proteins have been co-crystallised with nucleotide. Hung et al. [21] reported that the adenine base interacted with Tyr16 of the histidine permease NBD, Smith et al. [22] reported the adenine base interacted with Tyr11 of MJ0796 NBD and Gaudet and Wiley [18] reported the adenine base interacted with Tyr512 of the human TAP1 NBD. De Azevedo et al. [12] reported that ring-A and ring-C of the flavonoid-type inhibitor *des*-chloroflavopiridol L868276 resembled the adenine base of ATP and underwent hydrophobic stacking interactions with Phe82 of cyclin dependant kinase 2. However, cyclin dependant kinase 2 and ABCB1 are evolutionarily diverse in terms of both sequence and structure, and pairwise alignment between the cyclin dependant kinase 2 and ABCB1 revealed no significant homology. Whilst similar bilobal architecture exists within both structures, the overall domain organisation is starkly different, with a lack of similarity in consensus sequence residues, such as the P-loop, which interact with the nucleotide. This may account for the apparent differences in binding modes in ABCB1 and cyclin dependant kinase 2 NBDs.

With many of the flavonoids studied, potential interactions of the carbonyl oxygen of the flavonoid with residues within the ABCB1 NBD2 P-loop was evident. The positioning of the carbonyl oxygen within the P-loop (irrespective of the orientation of the flavonoid within the NBD) was akin to the position of the α- and/or β-phosphate oxygen(s) of ATP within the P-loop, as illustrated by Hung et al. [21]. Docking of an ATP molecule into our model predicted residues within the P-loop (Ser1072-Ser1077) undergo hydrogen bonding with the β-phosphate oxygen of ATP (data not shown). This highlights a consistency with the amino acids reported to be involved in interactions with the β-phosphate oxygen atoms of ATP [18,21,22].

The precise mechanisms of interaction between flavonoid and ABCB1 NBD2 are unknown. A molecular model of the human ABCB1 NBD2 has been generated, using the X-ray crystallographic structures of ABC protein NBDs as structural templates, and the potential binding modes of flavonoids within the ABCB1 NBD2 are illustrated for the first time using a Lamarckian Genetic Algorithm and molecular docking studies. The results obtained from our studies illustrate a good correlation between predicted docking energy and in vitro interaction kinetics, despite the lack of N-terminal amino acids within the recombinant murine Abcb1 NBD2 construct. Our docking studies have highlighted the importance of Tyr1044 in NBD–flavonoid interaction, and alkylation at position 6 of ring-A (flavones and flavonols) and position 4 of ring-B (chalcones) in potentially providing positive stabilisation effects for binding. Thus, a homology model of ABCB1 NBD2 has proved useful in increasing our understanding on the potential mechanisms of interaction between flavonoids and NBD.

4. Conclusion

An ability to undertake in silico analyses of molecular interactions at the level of the NBD is extremely useful for understanding ligand–protein interactions and has obvious application to structure-based drug design. Indeed, this technique has recently been employed to identify and characterise the location of the binding sites of CFTR activators and to examine NBD-activators (including some flavonoids) at the NBD [34].

The human ABCB1 transporter is able to influence the pharmacokinetic characteristics of therapeutic drugs and contributes to the phenomenon of MDR in cancer cells. As such, this transporter represents a potentially important therapeutic target in disease treatment. A better understanding of the mechanism of interaction of flavonoids with ABCB1 NBD2 may allow the rational development of compounds that would target ABCB1 NBD2 in an intervention strategy to increase the efficacy of drug-based treatments.

5. Experimental protocols

5.1. Model design

Templates for modelling were obtained from a BLAST [35] search and crystallographic structures obtained from the Protein Data Bank [36]. Multiple sequence alignments for homology modelling were generated using ClustalW [37]. The homology modelling software Modeller 6 (Version 2) [38] was used to generate a structure of the human ABCB1 NBD2 homologous to crystallographic structures of NBDs of ABC proteins. The loop-optimisation module within Modeller was used to refine loop-segments within ABCB1 NBD2. The optimal model was selected based on bond angle stereochemistry using PROCHECK [39] and subjected to 1000 steps of energy minimisation using Gromacs (Version 3.0) [40].

5.2. Docking simulation

Flavonoids were docked into ABCB1 NBD2 to determine the degree of correlation between predicted docking energy and published dissociation constants for flavonoids interacting at the NBD and to provide mechanistic information of flavonoid–NBD2 interaction. Docking of flavonoids was carried out using the Autodock 3.0.5 software [41]. Polar hydrogen atoms and partial atomic charges were assigned using the Amber force field, and atomic solvation and fragmental volumes assigned using the Addsol package. Flexible ligand torsions were assigned using Autotors, with the protein remaining rigid during the simulation. For each atom within the ligands grid-maps of NBD2 were generated using Autogrid, with a grid-spacing interval of 0.375 Å centred upon the Walker A site with dimensions of $50 \times 50 \times 50$ Å. An adaptive global–local search method, based upon the Lamarckian Genetic Algorithm, was

used for the scoring algorithm in docking studies due to its general robustness at reproducing crystallographic ligand placement [41]. Default docking parameters were employed throughout the study with the exception of: 100 runs per ligand with 2,000,000 energy evaluations per run. Ligand orientations were clustered into groups with a 0.5 Å cut-off. For flavonoids with larger substituent groups (butyl or greater) a 2 Å cut-off was selected.

A final docked representation of the potential binding mode of flavonoids was chosen based on the selection of the compound possessing the lowest docked energy within the most populated cluster of lowest possible energy.

Hydrogen bonding and hydrophobic interactions between docked flavonoids and amino acid residues within the ABCB1 NBD2 model were analysed using LigPlot (Version 1.0) [42]. Molecular surface representations were generated with Visual Molecular Dynamics [43]. The final docked energy value for each flavonoid examined is reported in the study.

References

[1] T.R. Stouch, O. Gudmundsson, Adv. Drug Deliv. Rev. 54 (2002) 315–328.
[2] C. Cordon-Cardo, J.P. O'Brien, J. Boccia, D. Casals, J.R. Bertino, M.R. Melamed, J. Histochem. Cytochem. 38 (1990) 1277–1287.
[3] World Health Organization, Life in the 21st century: a vision for all, WHO, Geneva, 1998.
[4] F.X. Mahon, M.W.N. Deininger, B. Schultheis, J. Chabrol, J. Reiffers, J.M. Goldman, J.V. Melo, Blood 96 (2000) 1070–1079.
[5] V. Sandor, T. Fojo, S.E. Bates, Drug Resist. Updat. 1 (1998) 190–200.
[6] M.C. de Jong, J.W. Slootstra, G.L. Scheffer, A.B. Schroeijers, W.C. Puijk, R. Dinkelberg, M. Icool, H.J. Broxterman, R.H. Meloen, R.J. Scheper, Cancer Res. 61 (2001) 2552–2557.
[7] P.M. Jones, A.M. George, FEMS Microbiol. Lett. 179 (1999) 187–202.
[8] P. Manavalan, D.G. Dearborn, J.M. McPherson, A.E. Smith, FEBS Lett. 1 (1995) 87–91.
[9] Y.R. Yuan, S. Blecker, O. Martsinkevich, L. Millen, P.J. Thomas, J.F. Hunt, J. Biol. Chem. 34 (2001) 32313–32323.
[10] E. Middleton Jr., C. Kandaswami, T.C. Theoharides, Pharmacol. Rev. 52 (2000) 673–751.
[11] M. Hagiwara, S. Inoue, T. Tanaka, K. Nunoki, M. Ito, H. Hidaka, Biochem. Pharmacol. 37 (1988) 2987–2992.
[12] W.F. De Azevedo, H. Mueller-Dieckmann, U. Schulze-Gahmen, P.J. Worland, E. Sausville, S.H. Kim, Proc. Natl. Acad. Sci. USA 93 (1996) 2735–2740.
[13] T. Akiyama, J. Ishida, S. Nakagawa, H. Ogawara, S. Watanabe, N. Itoh, J. Biol. Chem. 262 (1987) 5592–5595.
[14] F. Sicheri, I. Moarefi, J. Kuriyan, Nature 385 (1997) 602–609.
[15] M.J. Robinson, A.H. Corbett, N. Osheroff, Biochemistry 32 (1993) 3638–3643.
[16] L. Nissler, R. Gebhardt, S. Berger, Anal. Bioanal. Chem. 379 (2004) 1045–1049.
[17] M.F. Rosenberg, R. Callaghan, S. Modok, C.F. Higgins, R.C. Ford, J. Biol. Chem. 280 (2005) 2857–2862.
[18] R. Gaudet, D.C. Wiley, EMBO J. 20 (2001) 4964–4972.
[19] L. Schmitt, H. Benabdelhak, M.A. Blight, I.B. Holland, M.T. Stubbs, J. Mol. Biol. 330 (2003) 333–342.
[20] Y. Yuan, H. Chen, D. Patel, Crystal structure of lmra atp-binding domain reveals the two-site alternating mechanism at molecular level Protein Data Bank accession code: 1mv5.
[21] L.W. Hung, I.X. Wang, K. Nikaido, P.Q. Liu, G.F. Ames, S.H. Kim, Nature 396 (1998) 703–707.
[22] P.C. Smith, N. Karpowich, L. Millen, J.E. Moody, J. Rosen, P.J. Thomas, J.F. Hunt, Mol. Cell 10 (2002) 139–149.
[23] B. Rost, Protein Eng. 12 (1999) 85–94.
[24] C.A. Kemp, J.U. Flanagan, A.J. van Eldik, J.D. Marechal, C.R. Wolf, G.C. Roberts, M.J. Paine, M.J. Sutcliffe, J. Med. Chem. 47 (2004) 5340–5346.
[25] Y. Xu, H. Liu, C. Niu, C. Luo, X. Luo, J. Shen, K. Chen, H. Jiang, Bioorg. Med. Chem. 12 (2004) 6193–6208.
[26] C.X. Xue, R.S. Zhang, H.X. Liu, X.J. Yao, M.C. Liu, Z.D. Hu, B.T. Fan, J. Chem. Inf. Comput. Sci. 44 (2004) 1693–1700.
[27] G. Conseil, H. Baubichon-Cortay, G. Dayan, J.M. Jault, D. Barron, A. Di Pietro, Proc. Natl. Acad. Sci. USA 95 (1998) 9831–9836.
[28] A. Boumendjel, F. Bois, C. Beney, A.-M. Mariotte, G. Conseil, A. Di Pietro, Bioorg. Med. Chem. Lett. 11 (2001) 75–77.
[29] H. de Wet, D.B. McIntosh, G. Conseil, H. Baubichon-Cortay, T. Krell, J. Jault, J. Daskiewicz, D. Barron, A. Di Pietro, Biochemistry 40 (2000) 10382–10391.
[30] A. Di Pietro, G. Conseil, J.M. Pérez-Victoria, G. Dayan, H. Baubichon-Cortay, D. Trompier, E. Steinfels, J.M. Jault, H. de Wet, M. Maitrejean, G. Comte, A. Boumendjel, A.M. Mariotte, C. Dumontet, D.B. McIntosh, A. Goffeau, S. Castanys, F. Gamarro, D. Barron, Cell. Mol. Life Sci. 59 (2002) 307–322.
[31] G. Comte, J. Daskiewicz, C. Bayet, G. Conseil, A. Viornery-Vanier, C. Dumontet, A. Di Pietro, D. Barron, J. Med. Chem. 44 (2001) 763–768.
[32] F. Bois, A. Boumendjel, A.-M. Mariotte, G. Conseil, A. Di Petro, Bioorg. Med. Chem. 7 (1999) 2691–2695.
[33] M. Maitrejean, G. Comte, D. Barron, K. El Khirat, G. Conseil, A. Di Pietro, Bioorg. Med. Chem. Lett. 10 (2000) 157–160.
[34] O. Morana, L.J.V. Galiettab, O. Zegarra-Moranb, Cell. Mol. Life Sci. 62 (2005) 446–460.
[35] National Centre for Biotechnology Information, http://www.ncbi.nlm.nih.gov/Entrez/.
[36] H.M. Berman, J. Westbrook, Z. Feng, G. Gilliland, T.N. Bhat, H. Weissig, I.N. Shindyalov, P.E. Bourne, Nucleic Acids Res. 28 (2000) 235–242.
[37] D. Higgins, J. Thompson, T. Gibson, J.D. Thompson, D.G. Higgins, T.J. Gibson, Nucleic Acids Res. 22 (1994) 4673–4680.
[38] M.A. Marti-Renom, A. Stuart, A. Fiser, R. Sánchez, F. Melo, A. Sali, Annu. Rev. Biophys. Biomol. Struct. 29 (2000) 291–325.
[39] R.A. Laskowski, M.W. MacArthur, D.S. Moss, J.M. Thornton, J. Appl. Crystallogr. 26 (1993) 283–291.
[40] E. Lindahl, B. Hess, D. Van der Spoel, J. Mol. Mod. 7 (2000) 306–317.
[41] G.M. Morris, D.S. Goodsell, R.S. Halliday, R. Huey, W.E. Hart, R.K. Belew, A.J. Olson, J. Comput. Chem. 19 (1998) 1639–1662.
[42] A.C. Wallace, R.A. Laskowski, J.M. Thornton, Prot. Eng. 8 (1995) 127–134.
[43] W. Humphrey, A. Dalke, K. Schulten, J. Mol. Graph. 14 (1996) 33–38.